

1. The Conventional Iwasawa-Taniguchi Effect

The Iwasawa-Taniguchi, or X-ray Baldwin effect describes the anti-correlation between the equivalent width (EW) of the neutral Fe K α fluorescence line and the underlying continuum (Iwasawa & Taniguchi 1993, ApJ 413, 15) in unobscured (e.g., Bianchi et al. 2007, A&A 467, 19) and moderately obscured (Ricci et al. 2014, MNRAS 441, 3622) AGN.

A popular explanation for this effect is an intrinsic luminosity-dependent covering factor of the torus (see left panel). If the reprocessed spectrum (pink dotted, conventionally including the Fe K α line) is sub-dominant relative to the direct transmitted component (purple dashed), then this decrease in covering factor reduces the strength of reprocessing and hence the iron line, relative to the transmission-dominated spectrum.

This is not expected in Compton-thick AGN, where the reprocessed spectrum is not sub-dominant over the transmitted component. The fluorescence and underlying reflection continuum are thus expected to scale together for Compton-thick AGN. However, here we present the first study into the Iwasawa-Taniguchi effect for Compton-thick AGN (for more details, see Boorman et al. 2018, MNRAS 477, 3775).

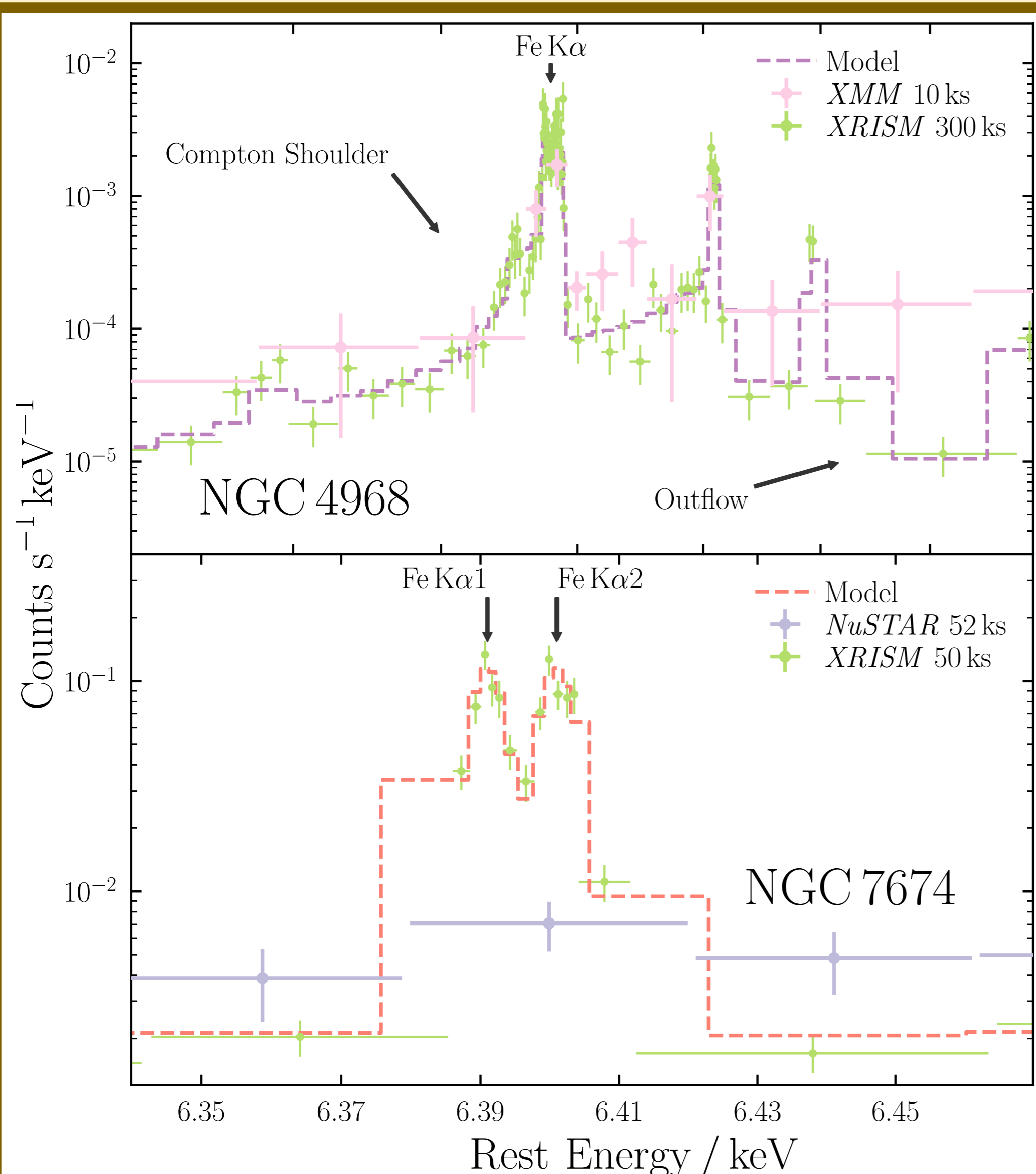
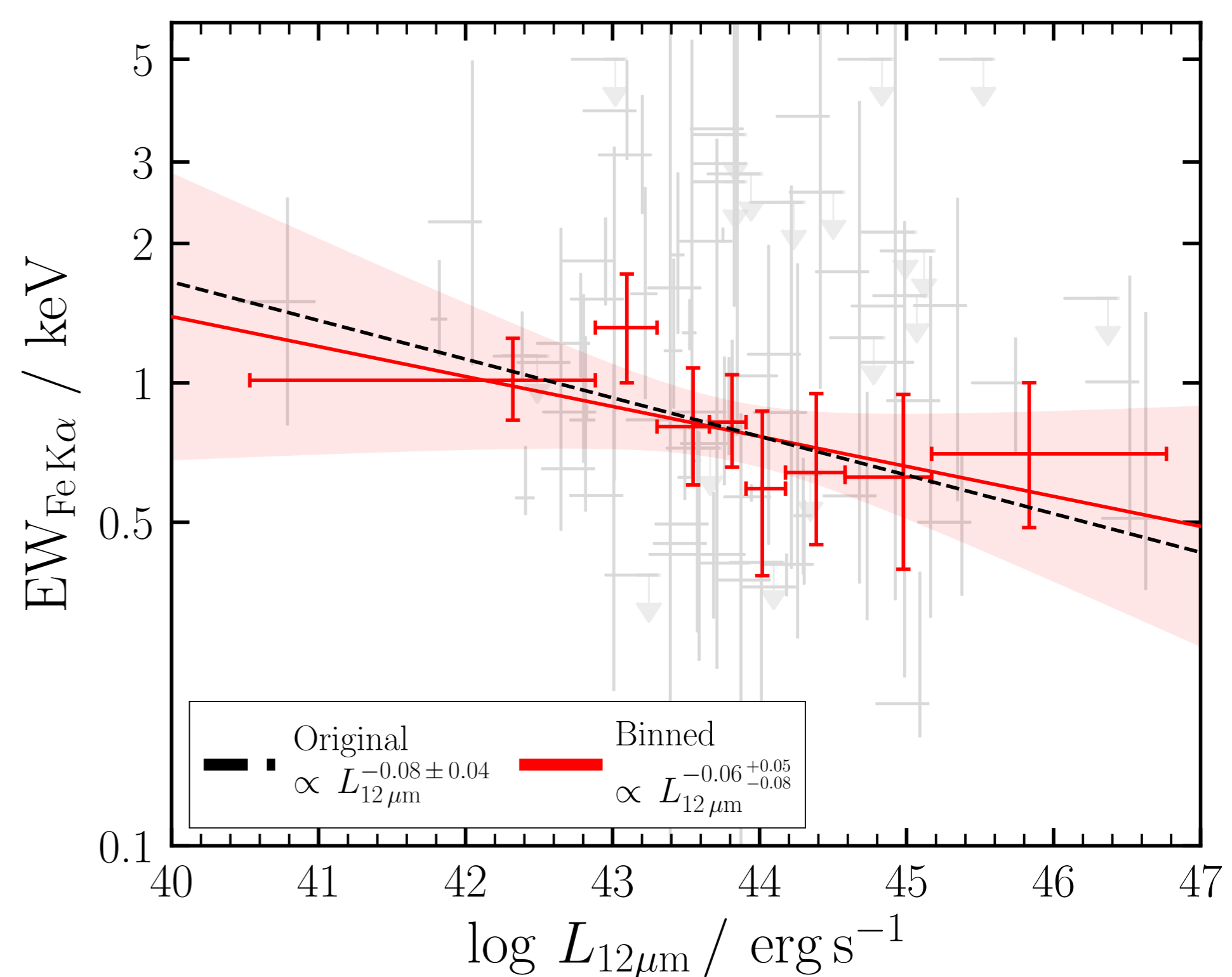
2. The Compton-thick Iwasawa-Taniguchi Effect

We confirmed 72 Compton-thick candidates with $z = 0.0014\text{--}3.7$ from the literature based on an observed offset from the $L_{12\mu\text{m}}$ (IR) vs. $L_{2-10\text{keV}}$ (X-ray) correlation from Asmus et al. (2015, MNRAS 454, 766). A decreased observed X-ray luminosity relative to the IR is expected for Compton-thick AGN.

Next we used the 12 μm luminosity as a proxy for the AGN bolometric luminosity, and derived the rest-frame EW from phenomenological X-ray spectral fits. With a bootstrapped fitting procedure, we were then able to confirm an anti-correlation to 98.7% significance. The linear fit to unbinned and binned data are shown in black and red on the right, respectively.

We identified several explanations for such an effect: a current lack of high-redshift reflection-dominated Compton-thick AGN, obscuration arising from the Broad Line Region (e.g., Gandhi, Hönicg & Kishimoto, 2015 ApJ 812, 113), dilution by a diffuse ionized mirror of gas (e.g., Matt & Iwasawa 2019, MNRAS 482, 151), unresolved dual AGN and anisotropic scattering effects of dust grains on X-ray photons (e.g., Gohil & Ballantyne MNRAS 449, 1449).

If confirmed on larger samples, this could implicate current models to underpredict intrinsic luminosities and growth rates by up to two dex.



3. XRISM/Resolve

Conventional methods for observing X-ray photons with CCDs feature spectral resolution $E/\Delta E < 50$ in the 5–8 keV energy range. Obscured AGN imprint many clues to their obscuration in this range with iron fluorescence (e.g., Lightman & White 1988 ApJ 335, 57), and the majority of current instrument resolutions are insufficient to fully resolve most of these. XRISM (launch date 2021, Guainazzi & Tashiro 2018 arXiv:1807.06903) features a revolutionary microcalorimeter – ‘Resolve’ – which will deliver a supreme resolution of $E/\Delta E > 1000$.

Two Compton-thick AGN spectra are simulated with XRISM exposures in the left figure. The upper panel shows a simulation of NGC 4968 – a relatively faint Compton-thick AGN with extreme Fe K α emission (LaMassa et al. 2017 ApJ 835, 91). XRISM fully resolves the ‘Compton Shoulder’ redward of the 6.4 keV line core – capable of constraining the geometry of AGN obscurers (e.g., Odaoka et al. 2016 MNRAS 462, 2366). The bottom panel shows a simulation of NGC 7674 – a median X-ray flux Compton-thick AGN with the weakest Fe K α line of any local Compton-thick AGN known (Boorman et al. 2016 ApJ 833, 245). Despite being weak, XRISM fully resolves the Fe K α doublet into its two separate components – an impossible feat with all instruments to date. Such detailed line profiles will constrain broadening effects and line fluxes – critical for probing the geometry, dynamics and composition of AGN obscurers.